

Preliminary Observation of Parity Nonconservation in Atomic Thallium

R. Conti, P. Bucksbaum, S. Chu, E. Commins, and L. Hunter

Physics Department, University of California, Berkeley, California 94720, and Materials and Molecular Research Science Division, Lawrence Berkeley Laboratory, Berkeley, California 94720

(Received 20 November 1978)

Parity nonconservation is observed in the $6^2P_{1/2}-7^2P_{1/2}$ transition in thallium. Absorption of circularly polarized 293-nm photons by $6^2P_{1/2}$ atoms in an E field results in polarization of the $7^2P_{1/2}$ state through interference of Stark $E1$ amplitudes with $M1$ and parity-nonconserving $E1$ amplitudes \mathfrak{M} and \mathcal{E}_p . Detection of this polarization yields the circular dichroism $\delta = +(5.2 \pm 2.4) \times 10^{-3}$, which agrees in sign and magnitude with theoretical estimates based on the Weinberg-Salam model.

We report preliminary observations of parity nonconservation (PNC) in the $6^2P_{1/2}-7^2P_{1/2}$ transition (292.7 nm) in atomic thallium (see Fig. 1). The transition is forbidden $M1$ with measured amplitude $\mathfrak{M} = (-2.1 \pm 0.3) \times 10^{-5} |e\hbar/2m_e c|$.¹ If parity is not conserved, the $6^2P_{1/2}$ and $7^2P_{1/2}$ states are admixed with $2^2S_{1/2}$ states. The transition amplitude then contains an additional $E1$ component \mathcal{E}_p , and circular dichroism exists, defined by

$$\delta = \frac{\sigma_+ - \sigma_-}{\sigma_+ + \sigma_-} = \frac{2 \operatorname{Im}(\mathcal{E}_p \mathfrak{M}^*)}{|\mathfrak{M}|^2 + |\mathcal{E}_p|^2} \approx \frac{2 \operatorname{Im}(\mathcal{E}_p)}{\mathfrak{M}}, \quad (1)$$

where σ_{\pm} are the cross sections for absorption of 293-nm photons with \pm helicity, respectively. Theoretical estimates of δ based on the Weinberg-Salem (W-S) model² yield^{3,4}

$$\begin{aligned} \delta_{\text{theor}} &= 2 \operatorname{Im}(\mathcal{E}_{p, \text{theor}}) / M_{\text{expt}} \\ &= (+2.3 \pm 0.9) \times 10^{-3} \end{aligned} \quad (2)$$

for $\sin^2\theta_W = 0.25$, where θ_W is the Weinberg angle. The uncertainty in δ_{theor} arises from the uncertainties in M_{expt} ($\sim 15\%$) and $\mathcal{E}_{p, \text{theor}}$ ($\sim 25\%$). The aim of this experiment is to measure δ .

Investigations of this type were first suggested by Bouchiat and Bouchiat,⁵ and their experiment on Cs is in progress.⁶ Also, optical-rotation experiments on bismuth have been reported (but with contradictory results),⁷⁻⁹ while PNC in high-energy electron scattering, consistent with the W-S model, has been observed.¹⁰

The simplest way to measure δ would be to illuminate Tl vapor in a field-free region with circularly polarized 293-nm light and observe the helicity dependence of the decay fluorescence (e.g., at 535 nm; see Fig. 1). Unfortunately this is impractical because of background effects. Instead, using a technique first suggested by Bouchiat and Bouchiat,⁵ we apply an external field \vec{E} which Stark mixes $2^2P_{1/2}$ states with $2^2S_{1/2}$ and

$2^2D_{3/2}$ states. The transition intensity, proportional to E^2 , is thereby increased above the background; moreover interference between the Stark transition amplitudes and the \mathfrak{M} and \mathcal{E}_p amplitudes polarizes the $7^2P_{1/2}$ state, permitting measurement of \mathfrak{M} and δ .

Let the 293-nm photon beam be along x , and choose $\vec{E} = E\hat{y}$ [see Fig. 1(b)]. Ignoring terms of order $[\mathfrak{M} \mp \mathcal{E}_p]^2$, we find the $7^2P_{1/2}$ polarization

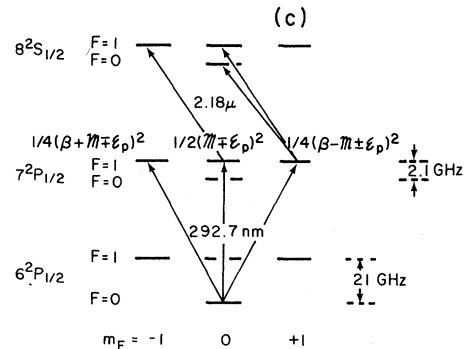
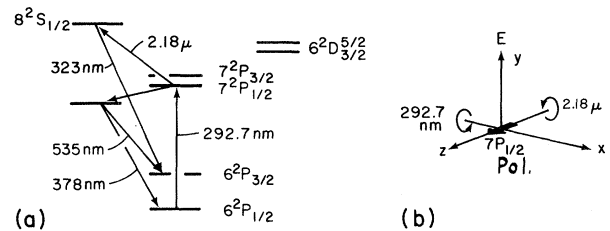


FIG. 1. (a) Low-lying energy levels of Tl (not to scale). (b) Coordinate system, orientation of photon beams, and electric field direction. (c) Schematic diagram indicating production and analysis of $7^2P_{1/2}$ polarization in the 0-1 transition. The rates at which the $F=1$, $m_F = -1$, 0, and $+1$ levels are populated in the $7^2P_{1/2}$ states are proportional to $\frac{1}{4}(\beta + \mathfrak{M} \mp \mathcal{E}_p)^2$, $\frac{1}{2}(\mathfrak{M} \mp \mathcal{E}_p)^2$, and $\frac{1}{4}(\beta - \mathfrak{M} \pm \mathcal{E}_p)^2$, respectively. The polarization is analyzed by circularly polarized 2.18- μm radiation ($7^2P_{1/2} - 8^2S_{1/2}$ transition). $8^2S_{1/2}$, hfs not resolved; $7^2P_{1/2}$, hfs is resolved.

along z to be

$$P_z(F=1 \rightarrow F=1) \approx \frac{4\alpha - 2\beta}{3\alpha^2 + 2\beta^2} [\mathfrak{M} \mp \mathcal{E}_p], \quad (3)$$

$$P_z(F=0 \rightarrow F=1) \approx \frac{-2}{\beta} [\mathfrak{M} \mp \mathcal{E}_p], \quad (4)$$

$$P_z(F=0 \rightarrow F=0) = 0, \quad (5)$$

for each indicated hfs component of the transition. Here \mp refer to ± 293 -nm photon helicities, and α and β are Stark amplitudes defined in Refs. 1 and 3. Calculations yield $\alpha = +7.4 \times 10^{-8} E$ and $\beta = 6.0 \times 10^{-8} E$ with uncertainties $\sim 15\%$ (atomic units, but E in volts per centimeter). This gives $\alpha/\beta = 1.23$, in agreement with observations.¹

In earlier measurements we detected P_z by observing the circular polarization P_c of 535-nm ($7^2S_{1/2} \rightarrow 6^2P_{3/2}$) fluorescence.¹ However P_c is very small ($P_c \approx 0.08P_z$) because of cascade depolarization and resonance trapping. In the present experiment we detect P_z by pumping the $7^2P_{1/2}$ atoms to the $8^2S_{1/2}$ state with 2.18- μm circularly polarized photons directed along z , and we observe the intensity of 323-nm ($8^2S_{1/2} \rightarrow 6^2P_{3/2}$) fluorescence. Let I_+ and I_- be the intensities for infrared (ir) photons with $J_z = \pm 1$. Then we observe the asymmetry

$$\Delta_0 = (I_- - I_+) / (I_- + I_+) = 0.7 P_z. \quad (6)$$

The dilution factor 0.7 is determined from measurements of \mathfrak{M} made during the PNC experiment. It agrees with a calibration experiment in which the 2.18- μm beam was directed along $-x$ to analyze the large polarization along that axis which arises from interference between the α and β amplitudes in the $F=1$ to $F=1$ transition,

$$P_x(1 \rightarrow 1) = \mp 4\alpha\beta / (3\alpha^2 + 2\beta^2) = \mp 0.75 \quad (7)$$

for \pm uv photon helicities, respectively.

Extensive measurements of absorption and polarization as a function of 2.18- μm power are in agreement with calculations. In normal operation the $7P$ - $8S$ transition is well saturated.

Figure 2 is a schematic diagram of the apparatus. L1 and L2 are synchronized flash-lamp-pumped, tunable, pulsed, dye lasers (pulse width 0.5 μs , repetition rate 19 per s, energy per pulse ~ 7 mJ, and wavelength 585.4 nm).¹¹ Light from L1 passes through an ammonium dihydrogen arsenate (ADA) doubling crystal where 292.7-nm photons are produced. The 293-nm energy per pulse is ~ 0.6 mJ in a bandwidth ≤ 1.2 Ghz. The linear polarization is precisely defined by a Glan-air prism and circular polarization is pro-

duced by a crystalline-quartz quarter-wave plate which rotates as shown in Fig. 2 to provide pulse-to-pulse alternation of photon helicity. The quarter-wave plate is antireflection coated, and great care is taken with its alignment to avoid possible systematic errors, as will be discussed in detail in a forthcoming publication. Light from L2 drives a Chromatix CMX4/IR optical parametric oscillator for production of linearly polarized ir photons. These are circularly polarized with either of two quartz quarter-wave plates which are alternately inserted in the ir beam. Thallium vapor at $T = 1050^\circ\text{K}$, density $n \approx 9 \times 10^{14} \text{ cm}^{-3}$ is contained in the main cell (Suprasil fused quartz) which has plane tantalum electrodes, separation 1 cm, to generate E . There are two interaction regions (1 and 2) at which the ir photons (with opposite J_z) intersect the uv beam. The 323-nm fluorescence signals I_1 and I_2 from regions 1 and 2 are detected separately. The quantity $(I_1 - I_2) / (I_1 + I_2)$ is almost independent of intensity fluctuations but is directly proportional to P_z . Extensive measurements show that there are no nonlinear or saturation effects in absorption of 293-nm photons.

In practice we confine ourselves to observation of the 0-1 and 0-0 lines at 300 V/cm in all PNC data, because $P_z(0-1)$ is relatively large, $P_z(0-0)$ should be 0, and neither line is as sus-

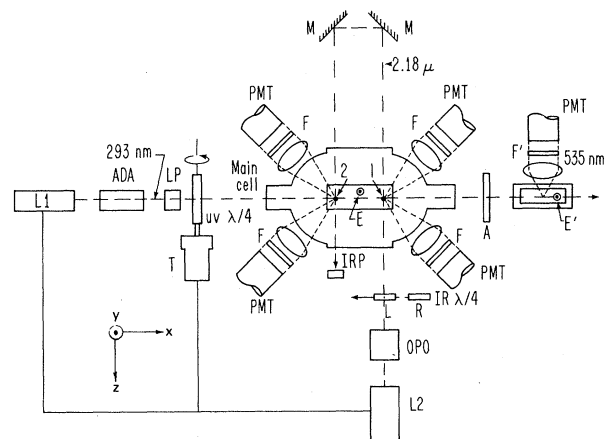


FIG. 2. Schematic diagram of PNC apparatus. L1, L2, flash-lamp-pumped pulsed dye lasers; ADA, doubling crystal; LP, linear polarizer; uv $\lambda/4$, rotating quarter-wave plate for 293 nm; T, drive motor and synchronizer for L1, L2; OPO, optical parametric oscillator to generate 2.18- μm photons; IR $\lambda/4$, 2.18- μm quarter-wave plates; F, interference filters and liquid filters for 323 nm; A, fixed uv quarter-wave plate; IRP, 2.18- μm infrared power monitor.

ceptible to possible systematic errors as is the 1-1 line. The choice of 300 V/cm is dictated by background, the major component of which is fluorescence at 323 nm from scattered 293-nm light. Extensive filtering in the detector channels has reduced this substantially. Lower values of E would not give larger measured asymmetries because of background dilution.

After traversing the main cell, the uv beam passes through a second fixed quarter-wave plate (A) which restores linear polarization $\hat{\epsilon}$. Since the uv helicity reverses with each pulse, $\hat{\epsilon}$ is alternately parallel to \hat{y} and to \hat{z} . The linearly polarized uv passes into a second cell with Stark field $\vec{E}' \parallel \vec{E}$. When $\hat{\epsilon} \parallel \hat{y}$ (\hat{z}) only the 0-0 (0-1) line is observed. This provides an effective means for tuning L1 to either desired resonance ($\Delta\nu = 2.13$ GHz) in the main cell. In practice our resolution is sufficient to give less than 10% contamination of either 0-0 or 0-1 line by the other.

The uv helicity alternates with each pulse, E is reversed after every second pulse, and the ir circular polarization changes sign after each set of 128 pulses. We define

$$\begin{aligned}\Delta_{1,2} &= (I_1 - I_2)/(I_1 + I_2) \quad (\text{regions 1, 2}), \\ \Delta' &= \frac{1}{2}[\Delta_{1,2}(E > 0) - \Delta_{1,2}(E < 0)] \quad (E \text{ reversal}), \\ \Delta &= \frac{1}{2}[\Delta'(\text{ir } +) - \Delta'(\text{ir } -)] \quad (\text{ir } CP \text{ reversal}).\end{aligned}$$

The average of observed asymmetries for opposite uv helicities (Δ_m) yields \mathfrak{M} , while one half

of the difference (Δ_p) yields \mathcal{E}_p . The 0-1 line is observed for 25 600 pulses, then an equal amount of data are taken for the 0-0 line. The entire procedure is executed repeatedly for a run.

Table I summarizes our results. Roughly equal amounts of data were taken with the ir beam entering region 1 first ("ir 1" in Table I) and entering region 2 first ("ir 2"). Also, approximately equal amounts were taken for the uv quarter-wave-plate assembly as shown in Fig. 2 ("uv +") and rotated about an axis normal to the page ("uv -"). A mirror placed before the fixed quarter-wave plate A may be used to reflect the 293-nm beam back into the main cell. In this case, the genuine PNC asymmetry is not affected, but the asymmetry Δ_m is reduced by a factor $(I - I')/(I + I')$ where I and I' are the direct and reflected 293-nm intensities, respectively. It is desirable to repeat the experiment in this manner but we have so far been prevented from acquiring a statistically significant amount of data for this case by difficulties in maintaining $I' \cong I$, in tuning to each resonance with greatly reduced signal in the second cell, and because of noise problems. A detailed description of the experiment and data to be published separately shows that imperfect circular polarization resulting from dichroism, optical activity, or Fresnel reflections in the uv quarter-wave plate can give a false Δ_p arising from \mathfrak{M} , but this is approximately the same in magnitude and sign for $\Delta_p(0-0)$ and $\Delta_p(0-1)$,

TABLE I. Summary of PNC data. All quoted uncertainties are standard errors of the mean. $E = 300$ V/cm for all data.

Condition	No. of pulses ($\times 10^6$)	Δ_m^a ($\times 10^{-7}$)	$\bar{\Delta}_{0-1}^b$ ($\times 10^{-7}$)	$\bar{\Delta}_{0-0}^b$ ($\times 10^{-7}$)	$\bar{\Delta}_D = \langle \bar{\Delta}_{0-1} - \bar{\Delta}_{0-0} \rangle^{b,c}$ ($\times 10^{-7}$)
uv+, ir 1	3.66 (54 h)	46350	-76 ± 113	185 ± 134	-265 ± 171
uv-, ir 1	3.37 (49 h)	44890	(-)64 ± 189	(+)11 ± 135	(-)101 ± 164
uv+, ir 2	3.99 (58 h)	-43860	(+)151 ± 113	(+)181 ± 95	(-)54 ± 128
uv-, ir 2	3.58 (52 h)	-41640	-324 ± 154	-41 ± 131	-279 ± 158
					$\bar{\Delta}_D = -169 \pm 74$

^aUncorrected $M1$ asymmetry. The statistical uncertainty in $\bar{\Delta}_m$ in any given run is $\sim 150 \times 10^{-7}$. The much larger variations shown are due to changes from run to run in signal-to-background ratio and slight variation in 2.18- μm circular polarization.

^bPNC asymmetries, normalized to $|\bar{\Delta}_m| = 55\,000 \times 10^{-7}$. The signs with parentheses indicate adjustment of sign to correct for changes in condition (column 1).

^c $\bar{\Delta}_D$ corrected ($\sim 6\%$) for the contamination of 0-0 line by 0-1 line. The apparent discrepancy between $\bar{\Delta}_D$ and $\bar{\Delta}_{0-1} - \bar{\Delta}_{0-0}$ arises because we divide the data into 32 small groups, calculate $\Delta_{0-1} - \Delta_{0-0}$ for each group, and take the weighted average to find $\bar{\Delta}_D$.

given our observation conditions. Thus we use $\Delta_D = \Delta_p(0-1) - \Delta_p(0-0)$ to determine δ . Detailed statistical analysis shows that fluctuations of $\Delta_D = \Delta_p(0-1) - \Delta_p(0-0)$ are smaller than individual fluctuations of $\Delta_p(0-1)$ or $\Delta_p(0-0)$. There is evidence for systematic drifts of $\Delta_p(0-1)$ and $\Delta_p(0-0)$ which are positively correlated and which have a time scale of hours, but these do not appear in Δ_D .

To obtain $\delta/2 = \text{Im} \mathcal{E}_p / \Re$ we take the ratio Δ_D / Δ_m' where $\Delta_m' = 1.17 \Delta_m$ and the factor 1.17 corrects for an estimated 8% reflection from the rear window of the main cell, which should diminish Δ_m but not Δ_D . We thus find

$$\delta_{\text{expt}} = +(5.2 \pm 2.4) \times 10^{-3}. \quad (8)$$

The uncertainty in this result is the standard error in the weighted mean, obtained as described in Table I, footnote c. The result is consistent in sign and magnitude with δ_{theor} given the uncertainty in the latter [see Eq. (2)]. From $\mathcal{E}_{p,\text{theor}} = (1.93i) \times 10^{-10} Q_W |e\hbar/2m_e c|$, with $Q_W = (1 - 4 \times \sin^2 \theta_W) Z - N$, we obtain $Q_W \approx -280 \pm 140$.

Experimental improvements now underway should permit a more precise determination of δ .

We thank Dr. M. Bouchiat, Dr. D. Neuffer, and Dr. M. Prior for helpful discussions, Miss P. Drell for much useful assistance, and Professor D. Shirley for administrative support. We are much indebted to glassblower D. Anderberg and

machinist G. Seiji for truly excellent workmanship. Three of us (R. C., P. B., and S. C.) were supported at various times during this research by National Science Foundation Fellowships. This work was done under the auspices of the Chemical Sciences Division, Office of Basic Energy Sciences, U. S. Department of Energy.

¹S. Chu, E. Commins, and R. Conti, *Phys. Lett.* **60A**, 96 (1977); S. Chu, Ph.D. thesis, Lawrence Berkeley Laboratory Report No. LBL-5731 (unpublished).

²S. Weinberg, *Phys. Rev. Lett.* **19**, 1264 (1967), and **27**, 1688 (1971), and *Phys. Rev. D* **5**, 1412 (1972); A. Salam, in *Elementary Particle Theory*, edited by N. Svartholm (Ålmqvist and Forlag, Stockholm, 1968).

³D. V. Neuffer and E. Commins, *Phys. Rev. A* **16**, 844 (1977).

⁴O. P. Sushkov, V. V. Flambaum, and I. B. Khirplovich, *Pis'ma Zh. Eksp. Teor. Fiz.* **24**, 461 (1976) [*JETP Lett.* **24**, 502 (1976)].

⁵M. A. Bouchiat and C. C. Bouchiat, *Phys. Lett.* **48B**, 111 (1974), and *J. Phys. (Paris)* **35**, 899 (1974), and **36**, 493 (1975).

⁶M. A. Bouchiat and L. Pottier, *J. Phys. (Paris)* **36**, L89 (1975), and **37**, L79 (1976).

⁷L. L. Lewis *et al.*, *Phys. Rev. Lett.* **39**, 795 (1977).

⁸P. E. G. Baird *et al.*, *Phys. Rev. Lett.* **39**, 798 (1977).

⁹L. M. Barkov and M. S. Zolotarev, *Pis'ma Zh. Eksp. Teor. Fiz.* **27**, 357 (1978) [*JETP Lett.* **27**, 379 (1978)].

¹⁰C. Y. Prescott *et al.*, *Phys. Lett.* **77B**, 347 (1978).

¹¹S. Chu and R. Smith, to be published.

Evidence for Axial-Vector and Pseudoscalar Resonances near 1.275 GeV in $\eta\pi^+\pi^-$

N. R. Stanton, P. Brockman, J. A. Dankowych, K. W. Edwards, J. Gandsman,^(a) D. Legacey, R. S. Longacre,^(b) J. F. Martin, P. M. Patel, A. J. Pawlicki,^(c) J. D. Prentice, E. Shabazian, T.-S. Yoon, and C. Zanfino^(d)

Department of Physics, The Ohio State University, Columbus, Ohio 43210, and Department of Physics, Carleton University, Ottawa, Ontario K1S 5B6, Canada, and Department of Physics, McGill University, Montreal, Quebec H3C 3G1, Canada, and Department of Physics, University of Toronto, Toronto, Ontario M5S 1A7, Canada

(Received 9 November 1978)

We present the first results from an isobar-model phase-shift analysis of the $\eta\pi^+\pi^-$ system. The $D(1275)$ meson is established as a narrow ($\Gamma \sim 10$ MeV) $IJ^P = 01^+$ resonance. Beneath the D is a broader ($\Gamma \sim 70$ MeV) $IJ^P = 00^-$ state which is a candidate for the radiatively excited η . The data are consistent with the existence of another 00^- object of comparable width near 1.4 GeV.

We present the first results from an isobar-model phase-shift analysis of the $\eta\pi^+\pi^-$ system, produced here in the reaction $\pi^-p \rightarrow \eta\pi^+\pi^-n$, with $\eta \rightarrow \gamma\gamma$, at 8.45 GeV/c. The observation of this final state rather than one with $\eta \rightarrow \pi^+\pi^-\pi^0$ has

the strong advantage of eliminating combinatorial backgrounds. The data were obtained at the Argonne National Laboratory zero-gradient synchrotron with the charged and neutral spectrometer, which detected both γ 's as well as the π^+ and π^- .